

# Report of JPL ITRS Combination Center

*presented by*  
*Richard S. Gross*

Jet Propulsion Laboratory  
California Institute of Technology  
Pasadena, CA 91109–8099, USA

International Earth Rotation and Reference Systems Service  
Directing Board Meeting No. 66

April 8, 2018  
Vienna, Austria

# Activities

- Correlations in ground deformation (Chin et al.)
  - Account for regional correlations in ground deformation
    - Caused by large-scale loading processes
    - By including statistics of regional deformation in stochastic model of process
    - Extending software to allow a full process noise matrix, not just diagonal
- Joint TRF/EOP/CRF Determination (Soja et al.)
  - Kalman filter to determine CRF from VLBI-only data developed
    - Variability of radio source positions modeled as random walk
    - Soja et al., Tuesday April 10, 17:30–19:00, Hall X3, X3.65 (EGU2018-10854)
- JTRF2014 Analysis (Abbondanza et al.)
  - Continuing to write article for *IERS TN*
  - Continuing to develop capability to update JTRF2014 monthly
  - Time variable structure of VLBI-SLR scale difference
    - Abbondanza et al., Tuesday April 10, 09:15–09:30, Room G1 (EGU2018-3745)

# Kalman Filter for CRF Determination



EGU General Assembly

8–13 April 2018

# On the determination of a Kalman filter celestial reference frame and its application in VLBI analysis

B. Soja<sup>1</sup>, H. Krasna<sup>2,3</sup>, J. Böhm<sup>2</sup>, C. Jacobs<sup>1</sup>, R. Gross<sup>1</sup>

1. Jet Propulsion Laboratory, California Institute of Technology 2. Technische Universität Wien 3. Astronomical Institute, Czech Academy of Sciences

Contact:  
Benedikt Soja  
bsoja@jpl.nasa.gov  
@b\_soja



## Introduction

In this study, we use **Kalman filtering** for the creation of a **celestial reference frame** (CRF). Having time series of radio source coordinates instead of temporally constant coordinates is beneficial for radio sources that exhibit temporal variations, for example, caused by source structure effects. However, the vast majority of radio sources has been observed on only very few occasions. For these sources, the constant coordinate model is sufficient and considerably more efficient to compute. Therefore, **we compute our CRF in two steps**; First, we estimate a **constant** frame of more than 4000 radio sources and then feed the residuals of about 800 selected sources into our Kalman filter to compute a **time series** frame.

We evaluate the CRF solutions by applying them in the **VLBI analysis** and comparing the estimated Earth orientation parameters (EOP) and radio source coordinates among each other as well as to external data sets.

## Methodology

### Two-level approach:

#### Constant frame

- Least-squares adjustment
- Input: normal equations

#### Time series frame

- Kalman filter
- Input: residuals based on constant frame

- Single-session analysis to create normal equations
- Computation of **constant** frame (global solution)
- Apply constant frame in single-session analysis to estimate residuals
- Feed residuals into Kalman filter and smoother to create **time series** frame

**VLBI**  
Very Long Baseline Interferometry

### Advantages:

Most radio sources have been observed less than five times → **constant** model computationally very efficient

Some radio sources with excellent observational history but irregular behavior (e.g., source structure) → **time series** able to capture these non-linear effects

**Constant + time series** approach allows for a **complete** CRF, taking into account **non-linearity** of selected sources

## VLBI CRF solutions

1980 – 2016.5  
5446 IVS-VLBI sessions

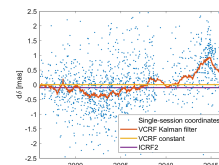


Nothnagel et al., 2015

**Constant frame:** 4097 radio sources

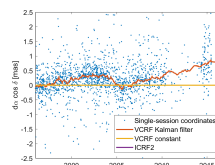
**Time series frame:** 822 radio sources  
295 used for datum definition

0119+115, declination



ICRF2 defining source

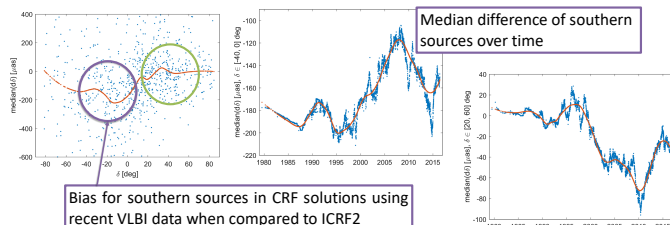
4C 39.25, right ascension



ICRF2 special handling source

## Source coordinates evaluation

### Investigating a temporal evolution of the “declination bias”

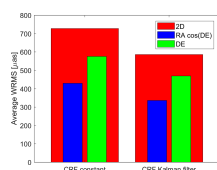


Bias for southern sources in CRF solutions using recent VLBI data when compared to ICRF2

For comparison, the same for northern sources

### Source coordinates in VLBI analysis

WRMS [μas]	RA cos(ΔE)	ΔE	2D
CRF constant	429	576	728
CRF Kalman filter	336	470	586
Δ(KF – constant)	-22%	-18%	-20%



“repeatability”

WRMS [μas]	RA cos(ΔE)	ΔE	2D
CRF constant	452	586	753
CRF Kalman filter	462	599	769
Δ(KF – constant)	+2%	+2%	+2%

estimated offsets

$$\hat{x} = x_0 + \Delta x$$

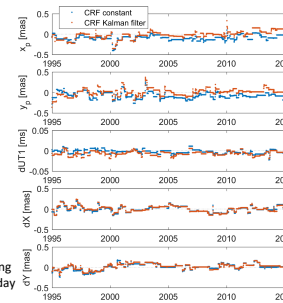
overall coordinates

a priori coordinates (from CRF)

## EOP evaluation

- Differences of EOP estimated in VLBI analysis w.r.t. IERS 14 C04 (plot & tables) and DTRF2014 EOP (tables)
- Similar results for EOP from ITRF2014 and JTRF2014 (not shown here)

Plotted: moving medians (30-day window)



Reference: IERS 14 C04

WRMS [μas]	x <sub>p</sub>	y <sub>p</sub>	dUT1	dX	dY
CRF constant	225	243	221	208	195
CRF Kalman filter	223	216	237	211	197
Δ(KF – constant)	-1%	-11%	+7%	+1%	+1%

WRMS [μas]	x <sub>p</sub>	y <sub>p</sub>	dUT1	dX	dY
CRF constant	209	211	217	208	194
CRF Kalman filter	214	215	222	211	196
Δ(KF – constant)	+2%	+2%	+2%	+1%	+1%

after subtracting trend

Reference: DTRF2014 EOP

WRMS [μas]	x <sub>p</sub>	y <sub>p</sub>	dUT1	dX	dY
CRF constant	221	216	690	377	377
CRF Kalman filter	225	221	691	377	380
Δ(KF – constant)	+2%	+2%	+0%	0%	+1%

WRMS [μas]	x <sub>p</sub>	y <sub>p</sub>	dUT1	dX	dY
CRF constant	243	240	691	378	378
CRF Kalman filter	226	219	693	377	380
Δ(KF – constant)	-7%	-9%	+0%	-0%	+1%

## Summary

- 2-level CRF:** complete **constant** frame, consistent with **time series** frame of well-observed sources (taking into account **non-linear** coordinate variations)
- Time series allows to study **time dependence of declination bias**
- Performance in VLBI analysis:** estimated coordinate offsets 20% smaller for Kalman filter CRF; repeatabilities of coordinates and EOP within a few percent

References:  
Nothnagel et al., 2015: The IVS data input to ITRF2014. International VLBI Service for Geodesy and Astrometry, GFZ Data Services. <http://doi.org/10.5880/GFZ.1.1.2015.002>  
Mayer et al., 2017: Tropospheric delay modelling and the celestial reference frame at radio wavelengths. *Astronomy & Astrophysics*, 606:A143

The authors would like to thank the IVS for observing, correlating and providing the VLBI data used in this work. B. Soja's research was supported by an appointment to the NASA Postdoctoral Program at the NASA Jet Propulsion Laboratory, administered by Universities Space Research Association under contract with NASA.



# VLBI-SLR Scale Difference

# Motivation

- Analysis of the scale difference between VLBI and SLR within the framework of **KALman filter for terrestrial REference Frame**.
- Dedicated study entirely focussed on the combination of VLBI and SLR only Space-Geodetic inputs (X,EOPs) along with local ties at VLBI-SLR co-located sites.
- As a result of the sequential nature of the algorithm, KALREF outputs a **time series of the quasi-instantaneous Helmert scale parameters** mapping VLBI's to SLR's scale.
- We provide and discuss the **time-variable** structure of the quasi-instantaneous scale difference between the 2 observing systems.

# The Input Data Set (from ITRF2014)

## Space-Geodetic Solutions

	Time Span	Sampling	SINEX	Constraints	EOPs
VLBI	1979.5 - 2015.0	$\approx$ 1-day	4792	None	PM,UT1,PMR,LOD
SLR	1983.0 - 1993.0	15-day	244	Loose	PM
	1993.0 - 2015.0	7-day	1148		

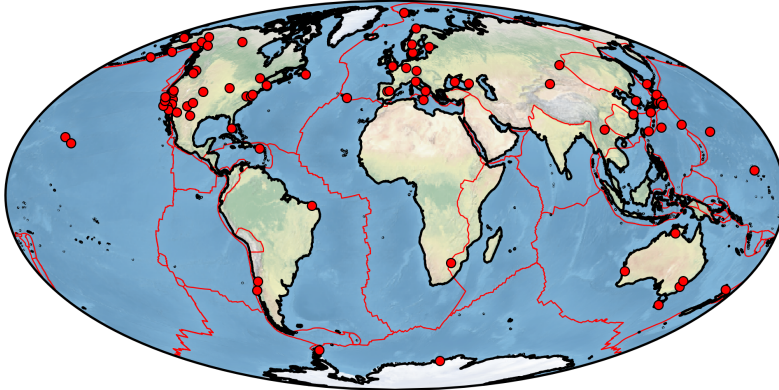
## Ground Site Ties

	Time Span	Sampling	SINEX	Constraints	EOPs
VLBI-SLR	1985.7 - 2014.2	Episodic	19	(Assumed) Minimal	None
SLR-SLR	–	Episodic	5	–	None
VLBI-VLBI	–	Episodic	2	–	None

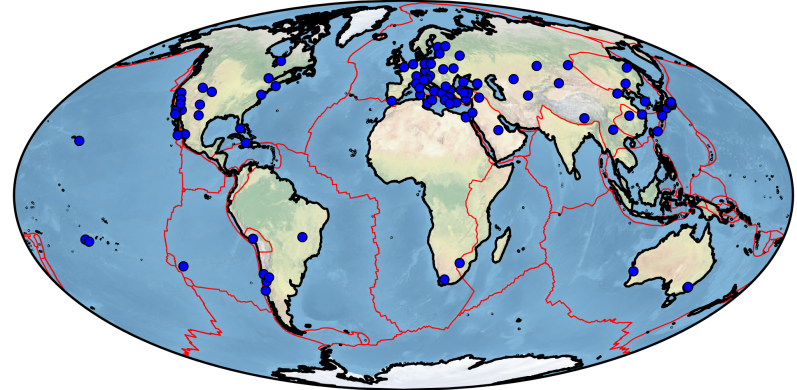
- 25 SLR-to-VLBI Tie Vectors
- 5 SLR-to-SLR Tie Vectors
- 7 VLBI-to-VLBI Tie Vectors
- Overall, **37** Tie Vectors

# VLBI and SLR Networks

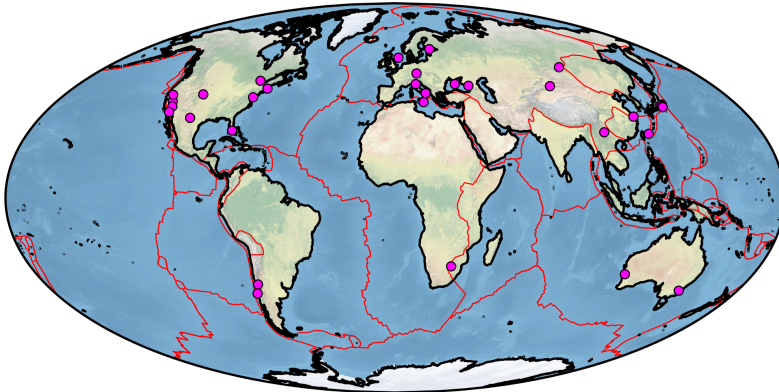
VLBI 104 Stations



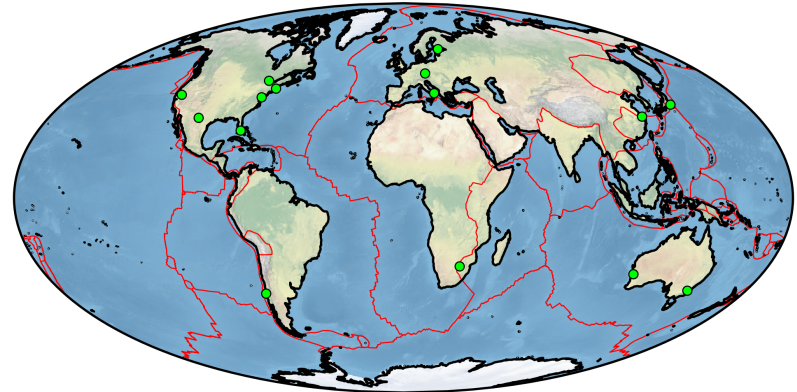
SLR 139 Stations



32 VLBI–SLR Co–Located Sites



15 VLBI–SLR Surveyed Sites





# Combination Setup

6 Different Solutions based on

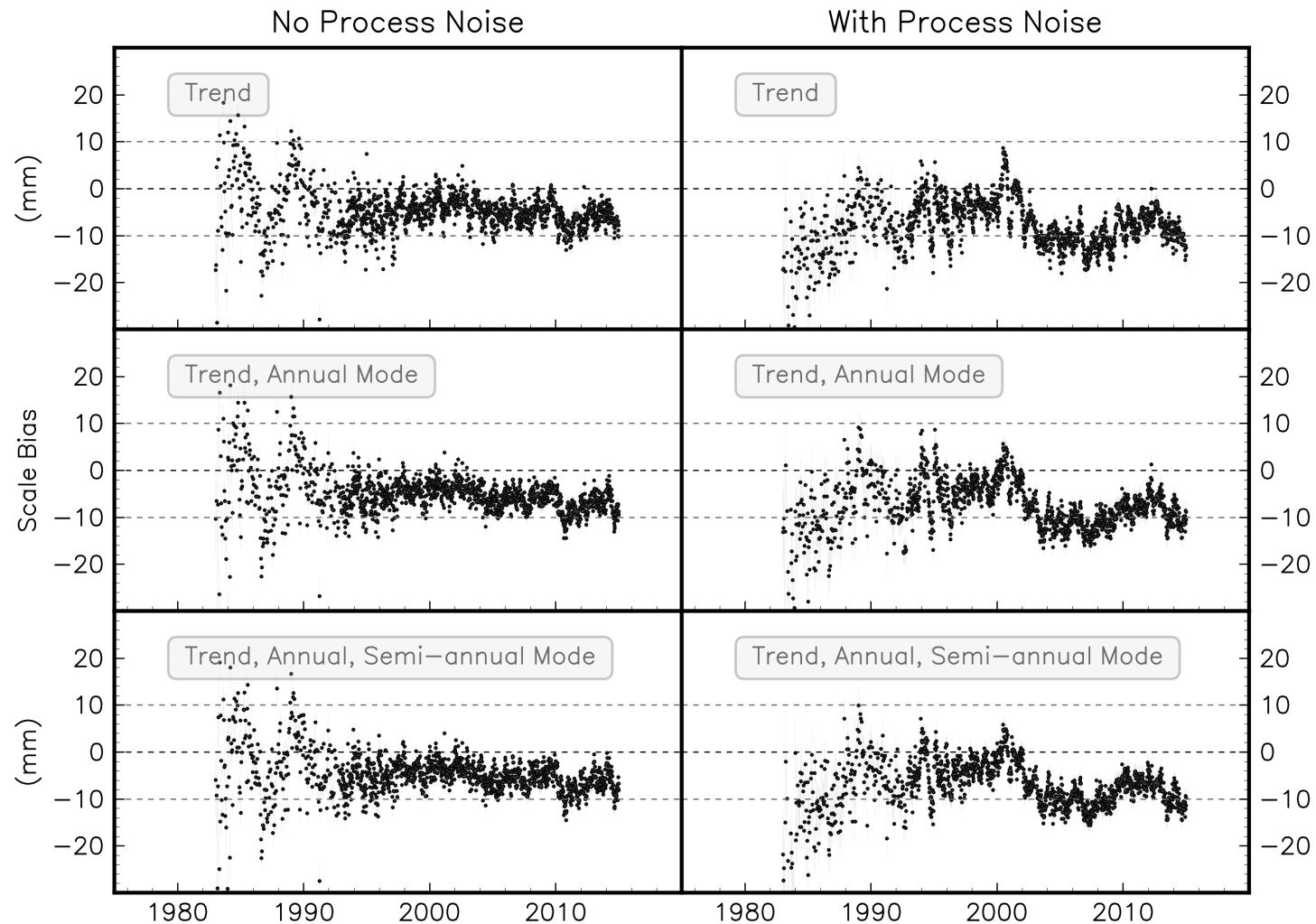
- 3 different station motion models
- with or without station-dependent position process noise

<b>Dataset</b>	SINEX Files from IVS,ILRS for ITRF2014
<b>Network</b>	243 Stations
<b>Segmentation</b>	from ITRF2014
<b>Station Motion Model</b>	Trend
	Trend, Annual
	Trend, Annual, and Semi-annual
<b>Process Noise</b>	None
	Station-Dependent Random Walk
<b>Origin</b>	Quasi-Instantaneous CM (SLR)
<b>Scale</b>	Quasi-Instantaneous VLBI
<b>Orientation</b>	No-Net-Rotation to ITRF2014

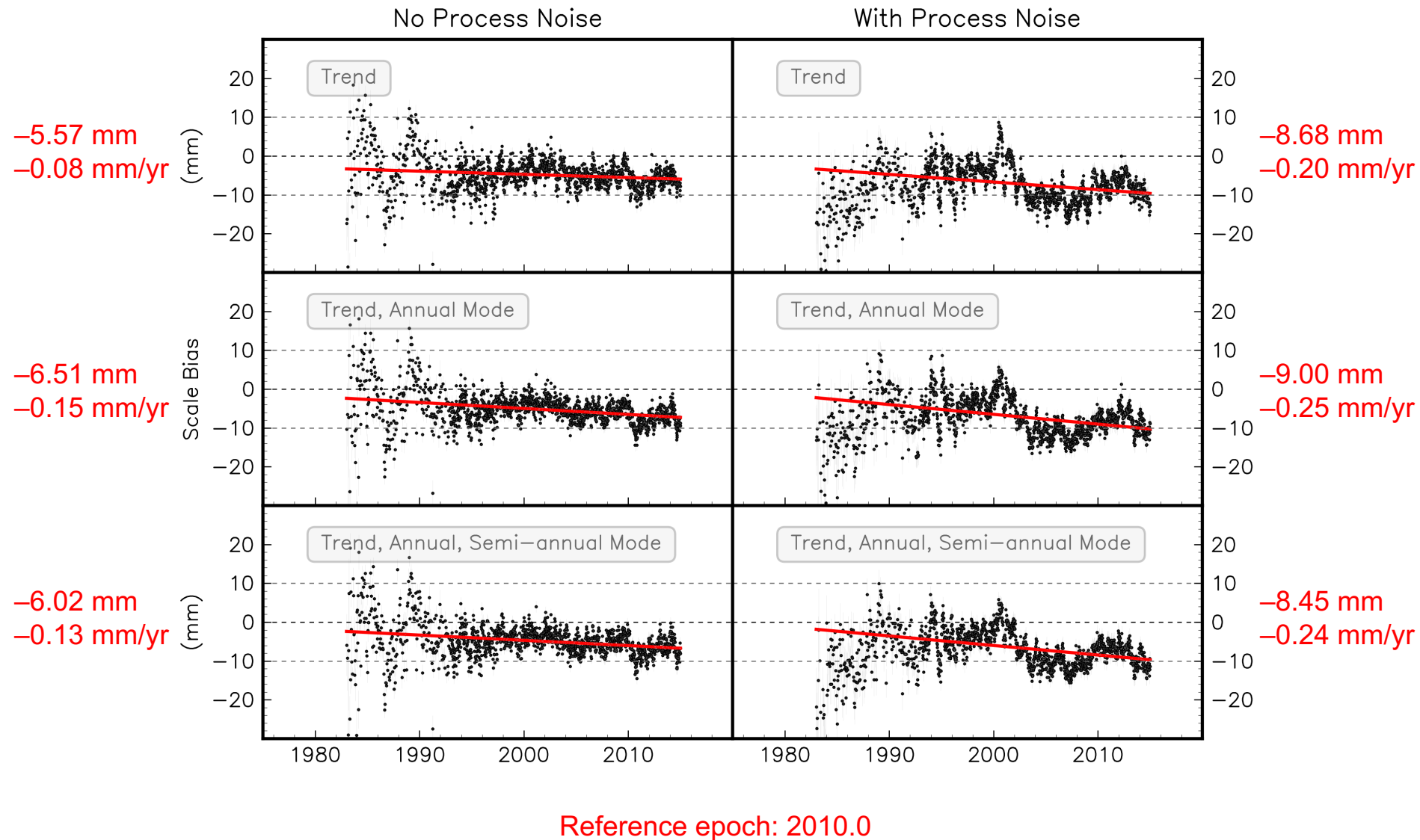
# Scaling of the Input Measurement Covariance Matrices

- **VLBI SINEX** Variance Factor =  $(2.98)^2$  (from JTRF2014 analyses)
- **SLR SINEX** Variance Factor =  $(2.61)^2$  (from JTRF2014 analyses)
- **Tie Vectors** - Two-step Procedure
  - **3-mm threshold Rescaling**  
Covariance matrices of tie vectors with formal nominal uncertainties smaller than 3 mm on any of the ENU baseline components are inflated.
  - **Iterative Rescaling** (via multiple KALREF runs)  
Covariance matrices of the tie vectors are iteratively rescaled until *normalized residuals* on all of the ENU components are less than 3.

# VLBI-to-SLR Scale Difference Time Series



# VLBI-to-SLR Scale Difference Time Series



# Key Facts about the VLBI-to-SLR Scale Differences

- Evidence of a **persistently negative scale bias** throughout the 6 configurations examined.
- According to the sign convention, a negative VLBI-to-SLR scale difference indicates that the baselines between VLBI stations must be contracted in order to match SLR's
- This is equivalent to state that VLBI baselines are on average larger than SLR's
- Biases and Drifts in the process noise-free configurations appear to be **consistent** with the results of Altamimi et al, who, on an equivalent data set, found an **SLR-to-VLBI bias** at 2010.0 of 1.02 ppb (6.5 mm) and a drift of 0.01 ppb/yr (0.06 mm/yr).